JOURNAL OF NATURAL PRODUCTS

pubs.acs.org/jnp

Article

Oxidized Juncuenin B Analogues with Increased Antiproliferative Activity on Human Adherent Cell Lines: Semisynthesis and Biological Evaluation

Csaba Bús,[‖] Ágnes Kulmány,[‖] Norbert Kúsz, Tímea Gonda, István Zupkó, Attila Mándi, Tibor Kurtán, Barbara Tóth, Judit Hohmann, Attila Hunyadi,* and Andrea Vasas*

Cite This: *J. Nat. Prod.* 2020, 83, 3250−3261

Read Online

ACCESS | Metrics & More | Article Recommendations | Supporting Information

ABSTRACT: Phenanthrenes have become the subject of intensive research during the past decades because of their structural diversity and wide range of pharmacological activities. Earlier studies demonstrated that semisynthetic derivatization of these natural compounds could result in more active agents, and oxidative transformations are particularly promising in this regard. In our work, a natural phenanthrene, juncuenin B, was transformed by hypervalent iodine(III) reagents using a diversity-oriented approach. Eleven racemic semisynthetic compounds were produced, the majority containing an alkyl substituted *p*-quinol ring. Purification of the compounds was carried out by chromatographic techniques, and their structures were elucidated by 1D and 2D NMR spectroscopic methods. Stereoisomers of the bioactive derivatives were separated by chiral-phase HPLC and the absolute configurations of the active compounds, 2,6-dioxo-1,8a-dimethoxy-1,7-dimethyl-8-vinyl-9,10-dihydrophenanthrenes (**1a**−**d**), and 8a-ethoxy-1,7-dimethyl-6-oxo-8-vinyl-9,10-dihydrophenanthrene-2-ols (**7a**,**b**) were determined by ECD measurements and TDDFT-ECD calculations. The antiproliferative activities of the compounds were tested on different (MCF-7, T47D, HeLa, SiHa, C33A, A2780) human gynecological cancer cell lines. Compounds **1a**−**d**, **4a**, **6a**, and **7a** possessed higher activity than juncuenin B on several tumor cell lines. The structure−activity relationship studies suggested that the *p*-quinol (2,5-cyclohexadien-4-hydroxy-1-one) moiety has a considerable effect on the antiproliferative properties, and substantial differences could be identified in the activities of the stereoisomers.

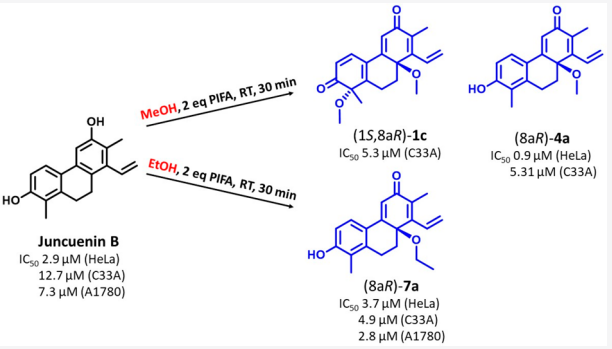

Phenanthrenes are a rather uncommon class of aromatic secondary metabolites and have a limited occurrence in nature. They are presumably formed by oxidative coupling of the aromatic rings of stilbene precursors.[1] Hitherto, more than 460 phenanthrenes, among them mono-, di-, and triphenanthrenes, were identified from different plant families, e.g., Orchidaceae, Juncaceae, Combretaceae, and Dioscoreaceae.[2] A large number of phenanthrenes with different substitution patterns have been reported with various pharmacological activities, such as antimicrobial, anti-inflammatory, cytotoxic, antiproliferative, spasmolytic, antiallergic, and anxiolytic effects.[2,3] The most thoroughly investigated denbinobin, a phenanthrenequinone, showed promising antiproliferative activity.[4−6] The mechanism of action of denbinobin involves caspase-dependent and caspase-independent apoptosis of colon cancer (COLO 205) cells.[4] Moreover, by enhancing the synthesis of reactive oxygen species (ROS), denbinobin induces apoptosis in Jurkat leukemia and human lung adenocarcinoma (A549) cells.[5,7] A structure−activity relationship study showed that the quinone substructure is required for enhancement of mitogen-activated protein kinase (MAPK)-independent ROS production activity.[5] Another phenanthrenequinone, calanquinone A, differing from denbinobin by the presence of an additional methoxy group, and synthetic phenanthrenequinones also possessed cytotoxic activity on different cell lines (HepG2, Hep3B, Ca9-22, A549, MCF-7, MDA-MB-231, MRC-5). Structure−activity relationship studies showed that intramolecular hydrogen bonding between the C-4 carbonyl and HO-5 in 3-methoxyphenanthrene-1,4-diones may be necessary for the cytotoxicity.[6]

The phenanthrene dehydroeffusol showed activity against two metastatic cancer cell lines, SGC-7901 (human gastric carcinoma) and AGS (human caucasian gastric adenocarcinoma) in a dose-dependent manner (IC_{50} 35.9 and 32.9 μM for

Received: May 5, 2020
Published: October 16, 2020

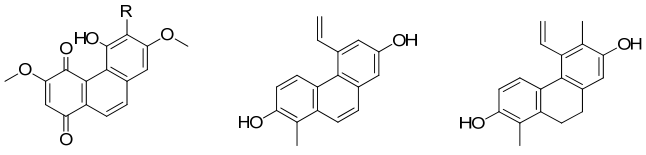

SGC-7901 and AGS cells, respectively). Gastric cancer cell mediated vasculogenic mimicry on SGC-7901 cells were also inhibited by this compound using the tube formation assay.[8] Dehydroeffusol effectively inhibited the gastric cancer cell invasion and migration without exerting significant acute toxicity.[9] Juncusol was observed to be cytotoxic on HeLa cells; treatment for 24 h increased the cell population in the G2/M and sub-G1 phases.[10] Juncuenin B possessed significant antiproliferative activity against different human tumor cell lines such as MDA-MB-231 (breast cancer), HeLa (cervical cancer), and A2780 (ovarian cancer) with IC_{50} values 9.4, 2.9, and 7.3 μM, respectively.[10]

The aim of this work was the semisynthetic modification of juncuenin B (1,7-dimethyl-8-vinyl-9,10-dihydrophenanthrene-2,6-diol) to prepare a variety of structurally related compounds with higher antiproliferative activities. The experimental approach was inspired by a 3-fold of reasons. First, the free radical scavenging-related, oxidized metabolites of phenolic compounds represent a chemical space particularly rich in bioactive compounds.[11] Second, we have recently demonstrated that the hypervalent iodine(III) reagent [bis-(trifluoroacetoxy)iodo]benzene (PIFA) may be efficiently used to obtain product mixtures rich in such oxidized scaffolds.[12] Third, the *p*-quinol moiety, anticipated from a PIFA-catalyzed oxidation of *p*-phenols, is the pharmacophore of several potent inhibitors of ATR-dependent signaling,[12,13] a crucial mechanism of DNA damage response that is an emerging antitumor target and a subject of many ongoing clinical studies.[14] Therefore, we followed a diversity-oriented semisynthetic approach using two hypervalent iodine reagents, PIFA, and (diacetoxyiodo)benzene (PIDA) to obtain oxidized derivatives of juncuenin B. Furthermore, various alcohols (MeOH, EtOH, and *n*-BuOH) were used as solvents to ensure formation of a set of differently substituted derivatives. Eleven chiral oxidation products (**1**−**11**), representing a wide structural diversity, were obtained in this way as racemates or stereoisomeric mixtures. Stereoisomers of the bioactive derivatives were resolved by chiral-phase HPLC and absolute configurations were assigned by ECD measurements and TDDFT-ECD calculations. The antiproliferative activity of the racemic compounds and separated optically active stereoisomers was investigated on MCF-7, T47D, HeLa, SiHa, C33A, and A2780 cell lines, which enabled us to establish both structure−activity and stereochemistry−activity relationships. In order to gain insight into their tumor selectivity, the compounds have also been tested on the NIH/3T3 cell line.

RESULTS AND DISCUSSION

Eleven racemic and enantiomerically pure chiral semisynthetic derivatives (**1**−**11**) (Scheme 1 and Figure 1) have been prepared from juncuenin B, a naturally occurring vinyl-substituted achiral dihydrophenanthrene, in five transformations (I−V) by hypervalent iodine(III) reagents using a diversity-oriented approach. PIFA and PIDA were used as

Scheme 1. Transformations of Juncuenin B under Different Conditions

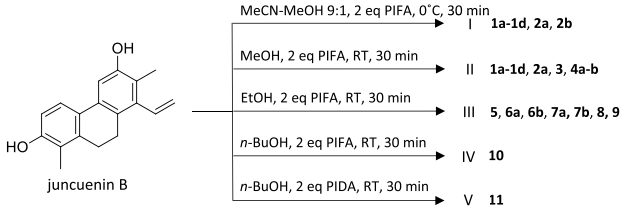

oxidants (PIFA in processes I−IV, PIDA in process V), under different conditions, in MeCN−MeOH (process I), MeOH (II), EtOH (III), *n*-BuOH (IV, V). PIFA and PIDA are well-known reagents for the oxidation of phenols leading to the formation of quinone-type products. This takes place through an aryloxyiodonium(III) intermediate forming a phenoxenium ion that undergoes a nucleophilic attack,[15] but PIFA and PIDA may also oxidize aromatic compounds via a single-electron transfer mechanism.[16] Following the oxidation, the mixture of products were subjected to solid-phase extraction on silica to remove the remaining oxidizing agent and the oxidation side-products. The purification process was followed by MPLC and HPLC.

During the reaction processes I−V, racemic mixtures of the compounds were formed, all of them bearing *p*- or *o*-quinol rings, substituted with methoxy-, ethoxy-, and *n*-butoxy groups based on the solvent used. In the case of reaction IV, only compound **10** could be isolated. It did not show structural analogy with the aforementioned compounds; therefore, the reaction was performed with PIDA under the same conditions (process V). This reaction yielded **11**, analogous to the compounds derived from **4** and **7**. As a result of chromatographic purifications, compounds with one stereogenic center were obtained as racemates (**3**, **4**, **7**−**11**), while compounds with two stereogenic centers were isolated as diastereomeric mixtures of two racemates (**1a**+**1d**, **1b**+**1c**, **2a**, **2b**, **6a**, **6b**). Separations of stereoisomers were performed using chiral-phase HPLC when the mixtures of stereoisomers or the racemates (**1a**−**d**, **4a**,**b**, **7a**,**b**) were found effective in the antiproliferative assay. This was done in order to compare the antiproliferative activity of the pure enantiomers and identify not only 2D structure−activity but also stereochemistry−activity relationships. The separation of the stereoisomers also enabled the characterization and determination of the absolute configurations of the bioactive derivatives by comparison of the experimental and TDDFT-calculated ECD spectra.

The structure determination was carried out by extensive spectroscopic analysis, using 1D and 2D NMR (^{1}H−^{1}H COSY, HSQC, and HMBC) spectroscopy and ECD data analysis.

In the NMR spectra of **1a**−**1d**, two sets of signals could be identified that were attributed to two racemic diastereomers **1a**+**1d** and **1b**+**1c** (ratio 1:1). The ^{1}H NMR spectrum of the **1a**−**1d** mixture showed the presence of a pair of isomeric compounds (**1a**+**1d** and **1b**+**1c**) as some signals were duplicated. Since these compounds are derived from juncuenin B, similar signals were found in the ^{1}H NMR spectrum: signals of two *o*-coupled aromatic protons (δ_H 6.24, d and 7.23, d/7.25, d), an aromatic proton singlet (δ_H 6.47/6.49), two methyls (δ_H 1.46, s and 2.08, s), a vinylic system at δ_H 6.58, dd, 5.83, dd, and 5.69, dd (H-13, H_2-14), and two methylene groups (δ_H 2.63, m, 1.68, m/1.67, m and δ_H 2.83, m, 2.57, dd). Two methoxy groups (δ_H 3.07, s and 2.92/2.93, s) were also

https://dx.doi.org/10.1021/acs.jnatprod.0c00499
J. Nat. Prod. 2020, 83, 3250−3261

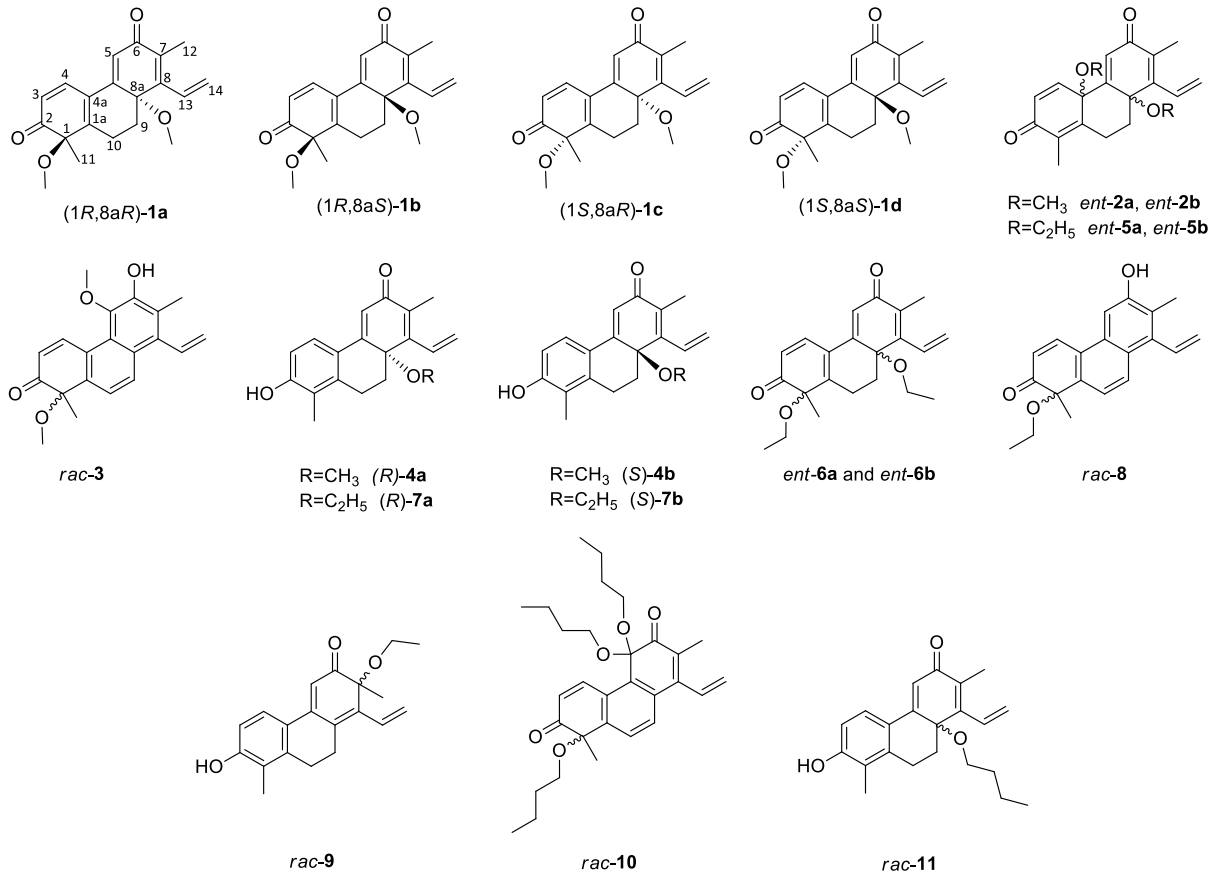

Figure 1. Structures of the prepared compounds **1**−**11**.

detected in the ^{1}H NMR spectrum (Table 1/**1a**+**d** and **1b**+**c**). The presence of two methylene signals (H_2-9, H_2-10) indicated this isomeric pair to be 9,10-dihydrophenanthrene derivatives. In the JMOD (*J*-modulated spin−echo experiment) spectrum, 20 carbon signals were displayed (Table 2/**1a**+**d** and **1b**+**c**). In the ^{1}H−^{1}H COSY spectrum, correlations were observed between δ_H 6.24, d and δ_H 7.23/7.25, d (H-3−H-4), between δ_H 2.63, m, 1.68/1.67, m and δ_H 2.83, m, 2.57, dd (H_2-9−H_2-10), and between δ_H 5.83, brd/5.69, dd and δ_H 6.58, dd (H-13−H_2-14) (Figure 2). The location of the methoxy groups was concluded from the HMBC spectra, as proton signal at δ_H 3.07 (CH_3O-1) showed correlations with δ_C 83.8 (C-1), whereas the signal at δ_H 2.92/2.93 (CH_3O-8a) correlated with δ_C 73.2 (C-8a) (Figure 2). Thus, the C-2 and C-6 hydroxy groups of juncuenin B were oxidized to carbonyl groups (δ_C 202.6 and 185.9, respectively) and methoxy-substituted dienone moieties were formed.

All of the above evidence confirmed the 2D structures of the **1a**−**1d** isomers (Figure 2).

The NMR spectra of the mixture of **1b**+**1c** were similar to those of **1a**+**1d**, only small differences were observed for the CH_3O-1, C-10, and C-11 resonances of **1a**+**1d** and **1b**+**1c**, which suggested that these compounds are structurally related to each other. Some ^{1}H and ^{13}C NMR signals were duplicated in the spectra of **1b**+**1c**, revealing the presence of a diastereomeric pair as for **1a**+**1d**.

After NMR studies the stereoisomers **1a**−**1d** were separated on a Lux amylose-1 chiral-phase column [t_R = 13.6 min (**1a**), 17.4 min (**1b**), 21.6 min (**1c**), and 23.6 min (**1d**)]. Experimental ECD spectra indicated mirror-image relationships between **1a**/**1d**, and **1b**/**1c**, respectively, verifying their enantiomeric relationships (Figure 3).

In order to elucidate the absolute configurations of **1a**−**d**, the solution TDDFT-ECD method was applied to (1*R*,8a*R*)-**1** and (1*R*,8a*S*)-**1**.[17] The initial Merck Molecular Force Field (MMFF) conformational search resulted in nine conformers for each in a 21 kJ/mol energy window, respectively. These geometries were reoptimized at the ωB97X/TZVP PCM/MeCN level[18] resulting in three conformers for both stereoisomers (Figures S8 and S9, Supporting Information). ECD spectra were computed at various levels and compared to the experimental spectra of **1a**−**1d**. There were only minor differences in the experimental ECD spectra of **1a** versus **1b** and **1c** versus **1d**, and the computed ECDs are mainly influenced by one of the two chirality centers. Boltzmann-averaged ECD data of both (1*R*,8a*R*)-**1** and (1*R*,8a*S*)-**1** gave acceptable to good agreement with the experimental data of **1a** and **1b** with the C-1 stereogenic center definitively influencing the ECD profile (Figure 4). Thus, the absolute configuration of this stereocenter could be determined as (1*R*) for the first- and second-eluted stereoisomers **1a** and **1b** and (1*S*) for the third- and fourth-eluting **1c** and **1d**. The shape of the B3LYP/TZVP PCM/MeCN and PBE0/TZVP PCM/MeCN ECD spectra of (1*R*,8a*R*)-**1** reproduced the experimental ECD curve of **1a** better, while those of (1*R*,8a*S*)-**1** were similar to the experimental spectrum of **1b** (Figure 5). The better agreements allowed tentative assignment (8a*R*) for **1a** and (8a*S*) for **1b**. DFT-NMR calculations of the B3LYP/6-31+G(d,p) conformers of (1*R*,8a*R*)-**1** and (1*R*,8a*S*)-**1** at the mPW1PW91/6-311+G(2d,p) level[19] could not differentiate

https://dx.doi.org/10.1021/acs.jnatprod.0c00499
J. Nat. Prod. 2020, 83, 3250−3261

Table 1. ^{1}H NMR (500 MHz) Data for Compounds 1−11[a]

	δ_H (J, Hz)													
position	**1a+d**	**1b+c**	**2a**	**2b**	**3**	**4a+b**	**5**	**6a**	**6b**	**7a+b**	**8**	**9**	**10**	**11**
3	6.24, d (10.2)	6.23, d (10.2)	6.45, d (9.9)	6.52, d (10.2)	6.30, d (10.6)	6.74, d (8.4)	6.40, d (9.9)	6.23, d (10.1)	6.21, d (10.1)	6.72, d (8.4)	6.32, d (10.4)	6.73, d (8.3)	6.21, d (10.6)	6.72, d (8.4)
4	7.23, d (10.2)/ 7.25, d (10.2)[b]	7.23, d (10.2)/ 7.25, d (10.2)[b]	6.61, d (9.9)	6.89, d (10.2)	9.06, d (10.6)	7.34, d (8.4)	6.66, d (9.9)	7.21, d (10.1)	7.21, d (10.1)	7.3, d (8.4)	8.18, d (10.4)	7.45, d (8.3)	8.71, d (10.6)	7.30, d (8.4)
5	6.47, s/ 6.49, s[b]	6.47, s/ 6.49, s[b]	6.84, s	6.45, s	–	6.58, s	6.82, s	6.43, s	6.45, s	6.54, s	7.49, s	6.42, s	–	6.55, s
9	1.68, m/ 1.67, m, 2.63, m[b]	1.68, m/ 1.67, m, 2.63, m[b]	1.92, m, 2.45, m	1.43, m, 2.59, m	8.19, d (8.8)	1.76, ddd (14.4, 11.3, 6.5), 2.69, dd (14.4, 5.7)	1.93, ddd (13.8, 10.0, 4.3), 2.47, m	1.62, m, 2.62, dd (14.0, 5.5)	1.66, m, 2.63, dd (13.9, 5.9)	1.74, ddd (13.9, 11.7, 6.5), 2.68, dd (14.0, 6.0)	8.15, d (8.8)	2.71, m[b]	7.62, d (8.3)	1.74, ddd (14.1, 11.6, 6.4), 2.68, dd (14.1, 5.8)
10	2.57, dd (20.2, 5.9), 2.83, m	2.50, dd (20.3, 6.0), 2.85, m	2.35, m, 2.83, m	2.67, m, 2.89, m	7.60, d (8.8)	2.75, dd (17.3, 6.5), 3.06, m	2.39, m, 2.87, ddd (13.8, 9.0, 4.3)	2.53, dd (14.4, 5.9), 2.88, ddd (16.5, 10.6, 5.5)	2.51, dd (20.4, 6.0), 2.86, ddd (20.2, 10.7, 6.0)	3.09, m, 2.74, dd (17.3, 6.2)	7.61, d (8.8)	2.84, m[b]	7.66, d (8.3)	2.73, dd (17.3, 6.4), 3.09, m
11	1.46, s	1.42, s	1.97, s	1.91, s	1.58, s	2.16, s	1.96, s	1.46, s	1.43, s	2.17, s	1.56, s	2.22, s	1.52, s	2.16, s
12	2.08, s	2.08, s	2.02, s	2.00, s	2.42, s	2.09, s	2.01, s	2.07, s	2.07, s	2.09, s	2.42, s	1.49, s	2.04, s	2.08, s
13	6.58, dd (17.8, 12.1)	6.58, dd (17.8, 12.1)	6.50, dd (17.9, 12.0)	6.51, dd (17.9, 11.9)	6.98, dd (17.9, 11.4)	6.63, dd (17.9, 11.9)	6.50, dd (17.8, 11.9)	6.61, dd (17.9, 11.9)	6.61, dd (17.9, 12.0)	6.65, dd (17.9, 11.9)	7.02, dd (17.7, 11.4)	6.67, dd (17.8, 11.8)	6.62, dd (17.9, 11.8)	6.64, dd (17.9, 11.9)
14	5.69, dd (12.1, 1.5), 5.83, dd (17.8, 1.5)	5.69, dd (12.1, 1.5), 5.83, dd (17.8, 1.5)	5.63, dd (12.0, 1.4), 5.78, dd (17.9, 1.4)	5.67, dd (11.9, 1.5), 5.70, dd (17.9, 1.4)	5.38, dd (17.9, 1.7), 5.82, dd (11.4, 1.7)	5,66, dd (11.9, 1.7), 5.85, dd (17.9, 1.7)	5.62, dd (11.9, 1.3), 5.80, dd (17.8, 1.3)	5.68, dd (11.9, 1.3), 5.87, dd (17.9, 1.3)	5.68, dd (12.0, 1.5), 5.89, dd (17.9, 1.5)	5.65, dd (11.9, 1.5), 5.89, dd (17.9, 1.5)	5.41, dd (17.7. 1.6), 5.84, dd (11.4, 1.6)	5.55, dd (11.8, 1.3), 5.87, dd (17.8, 1.3)	5.45, dd (17.9, 1.0), 5.82, d (11.8)	5.65, dd (11.9, 1.7), 5.89, dd (17.9, 1.7)

[a]Measured in $CDCl_3$. [b]Interchangeable. **1a+d**: CH_3O-1: 3.07, s; CH_3O-8a: 2.92, s/2.93, s (interchangeable with 1b); **1b+c**: CH_3O-1: 3.12, s; CH_3O-8a: 2.92, s/2.93,s (interchangeable with 1a); **2a**: CH_3O-4a: 3.04, s; CH_3O-8a: 2.72, s; **2b**: CH_3O-4a: 3.10, s; CH_3O-8a: 3.14, s; **3**: CH_3O-1: 3.08, s; CH_3O-5: 3.79, s; **4a+b**: CH_3O-8a: 2.85, s; **5**: C_2H_5O-4a (interchangeable with 8a): 2.76 dq (7.0, 14.1), 2.96, dq (7.0, 14.1) (CH_2), 0.80, t (7.0) (CH_3); C_2H_5O-8a (interchangeable with 4a): 3.08 dq (7.0, 14.1), 3.29, dq (7.0, 14.1) (CH_2), 1.11, t (7.0) (CH_3); **6a**: C_2H_5O-1 (interchangeable with 8a): 2.93, m, 3.36 dq (14.3, 7.1) (CH_2), 1.21, t (7.0) (CH_3); C_2H_5O-8a (interchangeable with 1): 2.91, m, 3.19 dq (14.3, 7.1) (CH_2), 1.01, t (7.0) (CH_3); **6b**: C_2H_5O-1:3.10, dq (14.2, 7.0), 3.34, dq (14.3, 7.1) (CH_2), 1.23, t (7.0) (CH_3); C_2H_5O-8a: 2.93, dq (14.2, 7.0), 3.17, dq (14.3, 7.1) (CH_2), 0.97, t (7.0) (CH_3); **7a+b**: C_2H_5O-8a: 2.92, m, 3.11, m (CH_2), 0.86, t (7.0) (CH_3); **8**: C_2H_5O-1: 3.00 dq (14.2, 7.0), 3.28 dq (14.2, 7.0) (CH_2), 1.20, t (7.0) (CH_3); **9**: C_2H_5O-7: 3.13, dq (13.9, 7.1), 3.26, dq (14.0, 7.1) (CH_2), 1.17, t (7.0) (CH_3); **10**: CH_3-$(CH_2)_3$-O-1: 3.22, m, 2.92, m (1′-CH_2), 1.58, m (2′-CH_2), 1.28−1.40, m (3′-CH_2), 0.87, t (7.4) (4′-CH_3); CH_3-$(CH_2)_3$-O-5: 3.14 m, 3.54, m (1″-CH_2), 1.47, m (2″-CH_2), 1.28−1.40, m (3″-CH_2), 0. 81, t (7.5)/0.83, t (7.5) (4″-CH_3) (interchangeable with 4‴-CH_3); 3.10, m, 3.45, m (1‴-CH_2), 1.47, m (2‴-CH_2), 1.28−1.40, m (3‴-CH_2), 0. 81, t (7.5)/0.83, t (7.5) (4‴-CH_3) (interchangeable with 4″-CH_3); **11**: CH_3-$(CH_2)_3$-O-8a: 2.83, m, 3.07, m (1′-CH_2), 1.13−1.23, m (2′-CH_2), 0.86−1.03, m (3′-CH_2), 0.62, t (7.4) (4′-CH_3).

https://dx.doi.org/10.1021/acs.jnatprod.0c00499
J. Nat. Prod. 2020, 83, 3250−3261

Table 2. ^{13}C NMR (125 MHz) Data for Compounds 1−11[a]

	δ_C type													
position	1a+d	1b+c	2a	2b	3	4a+b	5	6a	6b	7a+b	8	9	10	11
1	83.8, C	83.1, C	133.0, C	132.8, C	83.5, C	122.0, C	132.5, C	83.2, C	82.4, C	121.8, C	82.5, C	121.9, C	81.9, C	121.8, C
1a	157.2, C	157.0, C	150.9, C	154.4, C	145.1, C	133.9, C	152.0, C	157.9, C	157.5, C	139.1, C	144.2, C	141.0, C	147.3, C	139.2, C
2	202.6, C	202.4, C	185.4, C	184.7, C	202.4, C	155.8, CH	185.3, C	202.7, C	202.5, C	155.5, C	202.9, C	156.3, C	201.4, C	155.5, C
3	125.9, CH	125.9, CH	131.9, CH	131.8, CH	124.1, CH	113.8, CH	131.2, CH	125.8, CH	125.8, CH	113.7, CH	124.6, CH	114.2, CH	125.1, CH	113.6, CH
4	139.7, CH	139.7, CH	144.8, CH	146.5, CH	143. 6, CH	124.6, CH	145.6, CH	139.6, CH	139.6, CH	124.5, CH	139.8, CH	125.7, CH	142.7, CH	124.6, CH
4a	125.4, C	125.4, C	73.1, C	77.3, C	123.7, C	125.2, C	73.0, C	125.0, C	125.0, C	125.5, C	123.7, C	126.0, C	131.0, C	125.5, C
5	123.1, CH	123.1, CH	131.0, CH	128.8, CH	139.9, C	122.2, CH	130.6, CH	122.6, CH	122.6, CH	121.8, CH	103.3, CH	117.3, CH	94.6, C	121.7, CH
5a	151.9, C	151.9, C	159.6, C	156.8, C	122.9, C	156.7, C	160.5, C	152.7, C	152.9, C	157.7, C	130.7, C	150.6, C	136.1, C	157.8, C
6	185.9, C	185.9, C	186.2, C	186.1, C	147.8, C	186.5, C	186.3, C	185.9, C	186.0, C	186.6, C	154.0, C	202.6, C	194.4, C	186.7, C
7	135.8, C	135.8, C	134.1, C	133.9, C	125.2, C	135.7, C	133.8, C	135.2, C	135.3, C	135.1, C	124.4, C	82.1, C	130.4, C	135.1, C
8	149.6, C	149.6, C	150.2, C	153.6, C	134.1, C	149.6, C	150.7, C	150.2, C	150.4, C	150.6, C	138.2, C	145.9, C	147.9, C	150.5, C
8a	73.2, C	73.2, C	75.1, C	76.7, C	127.9, C	73.8, C	74.5, C	72.7, C	72.7, C	73.4, C	127.3, C	131.6, C	132.6, C	73.2, C
9	33.1/34.0, CH_2[b]	33.1/34.0, CH_2[b]	34.3, CH_2	41.1, CH_2	129.7, CH	34.5, CH_2	34.1, CH_2	33.2, CH_2	34.2, CH_2	34.8, CH_2	129.0, CH	25.8/26.6, CH_2[b]	129.0, CH	34.8, CH_2
10	21.8, CH_2	22.4, CH_2	22.8, CH_2	22.7, CH_2	121.3, CH	23.9, CH_2	22.9, CH_2	21.9, CH_2	22.5, CH_2	23.9, CH_2	121.0, CH	25.8/26.6, CH_2[b]	127.0, CH	23.9, CH_2
11	28.0, CH_3	26.6, CH_3	10.7, CH_3	10.9, CH_3	31.1, CH_3	11.2, CH_3	10.7, CH_3	27.2, CH_3	26.7, CH_3	11.2, CH_3	30.9, CH_3	11.3, CH_3	31.3, CH_3	11.2, CH_3
12	12.3, CH_3	12.3, CH_3	12.0, CH_3	12.3, CH_3	13.9, CH_3	12.3, CH_3	12.0, CH_3	12.2, CH_3	12.3, CH_3	12.3, CH_3	13.6, CH_3	28.2, CH_3	13.0, CH_3	12.3, CH_3
13	131.7, CH	131.7, CH	131.6, CH	132.0, CH	133.9, CH	132.1, CH	131.8, CH	131.9, CH	131.8, CH	132.2, CH	134.0, CH	131.2, CH	132.9, CH	132.2, CH
14	123.9, CH_2	123.9, CH_2	124.0, CH_2	124.0, CH_2	122.5, CH_2	123.3, CH_2	123.8, CH_2	123.7, CH_2	123.8, CH_2	123.3, CH_2	122.4, CH_2	121.7, CH_2	123.2, CH_2	123.3, CH_2

[a]Measured in $CDCl_3$. [b]Interchangeable. **1a+d**: CH_3O-1: 51.7; CH_3O-8a: 54.7; **1b+c**: CH_3O-1: 51.7; CH_3O-8a: 54.5; **2a**: CH_3O-4a: 51.1; CH_3O-8a: 52.5; **2b**: CH_3O-4a: 51.6; CH_3O-8a: 52.9; **7**: CH_3O-1: 54.4; CH_3O-5: 61.1; **4a+b**: CH_3O-8a: 51.6; **5**: C_2H_5O-4a (interchangeable with 8a): 60.2, CH_2, 14.7, CH_3; C_2H_5O-8a (interchangeable with 4a): 59.0, CH_2, 15.8, CH_3; **6a**: C_2H_5O-1 (interchangeable with 8a): 62.5, CH_2, 15.7, CH_3; C_2H_5O-8a (interchangeable with 1): 59.6, CH_2, 15.5, CH_3; **6b**: C_2H_5O-1: 62.2, CH_2, 15.8, CH_3; C_2H_5O-8a: 59.6, CH_2, 15.6, CH_3; **7a+b**: C_2H_5O-8a: 59.5, CH_2, 15.4 CH_3; **8**: C_2H_5O-1: 62.2, CH_2, 15.8, CH_3; **9**: C_2H_5O-7: 61.6, CH_2, 15.6, CH_3; **10**: CH_3-$(CH_2)_3$-O-7: 66.3 (1′-CH_2), 32.4 (2′-CH_2), 19.2/19.3/19.4 (3′-CH_2) (interchangeable with 3″-CH_2 and 3‴-CH_2), 14.1 (4′-CH_3); CH_3-$(CH_2)_3$-O-5: 63.3 (1″-CH_2), 31.8/31.9 (2″-CH_2) (interchangeable with 2‴-CH_2), 19.2/19.3/19.4 (3″-CH_2) (interchangeable with 3′-CH_2 and 3‴-CH_2), 13.8/13.9 (4″-CH_2) (interchangeable with 4‴-CH_3); 63.6 (1‴-CH_2), 31.8/31.9 (2‴-CH_2) (interchangeable with 2″-CH_2), 19.2/19.3/19.4 (3‴-CH_2) (interchangeable with 3′-CH_2 and 3″-CH_2), 13.8/13.9 (4‴-CH_2) (interchangeable with 4″-CH_3); **11**: CH_3-$(CH_2)_3$-O-8a: 63.5 (1′-CH_2), 31.9 (2′-CH_2), 19.1 (3′-CH_2), 13.7 (4′-CH_3).

https://dx.doi.org/10.1021/acs.jnatprod.0c00499
J. Nat. Prod. 2020, 83, 3250−3261

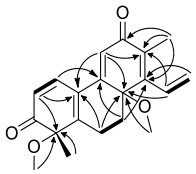

Figure 2. Diagnostic COSY (−) and HMBC (H → C) correlations of compounds **1a**−**d**.

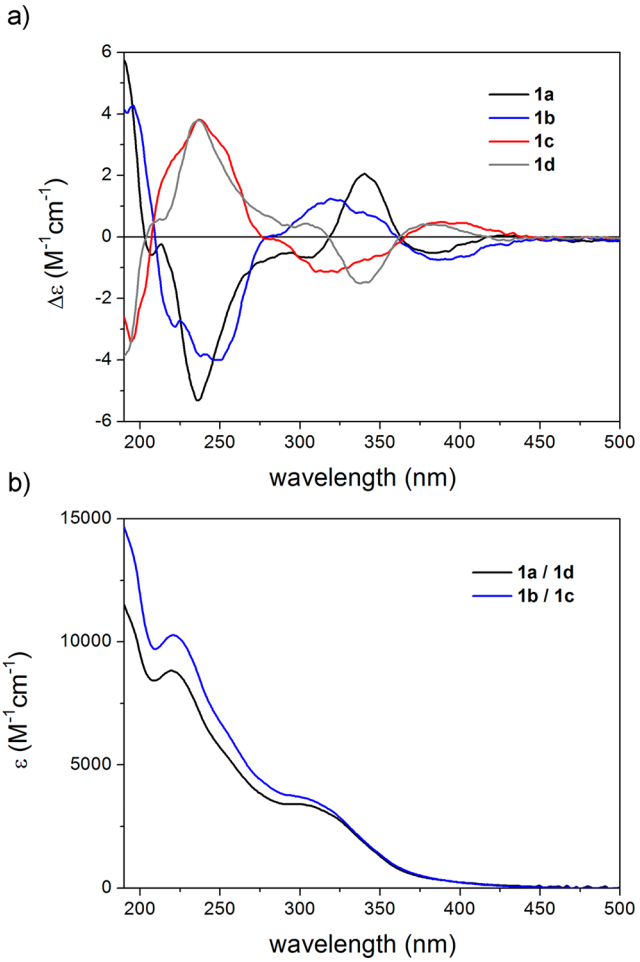

Figure 3. (a) Experimental ECD spectra of **1a**−**1d** in MeCN and (b) experimental UV spectra of **1a**/**1d** and **1b**/**1c** in MeCN.

the epimers due to the small chemical shift differences of the experimental values.[20]

The ^{1}H NMR spectrum of compound **2a** showed signals characteristic of juncuenin B analogues: signals of two *o*-coupled aromatic protons (δ_H 6.45, d and 6.61, d), one aromatic proton singlet (δ_H 6.84), two methyl singlets (δ_H 1.97 and 2.02), a vinyl group at δ_H 6.50, dd, 5.78, dd and 5.63, dd, two methylene groups (δ_H 1.92, m, 2.45, m, and δ_H 2.35, m, 2.83, m), and two methoxy singlets (δ_H 2.72 and 3.04), respectively (Table 1). In the JMOD spectrum, signals of 20 carbon atoms were detected (Table 2). In the ^{1}H−^{1}H COSY spectrum, correlations between δ_H 6.45, d and 6.61, d (H-3−H-4), between δ_H 2.35, m, 2.83, m, and δ_H 1.92, m, 2.45, m (H-9−H-10), and between δ_H 6.50, dd, and 5.78, dd, 5.63, dd (H-13−H_2-14) were observed. The position of the methyl groups were determined based on the HMBC correlations of the methyl protons at δ_H 1.97 and 2.02 with C-1 (δ_C 133.0)

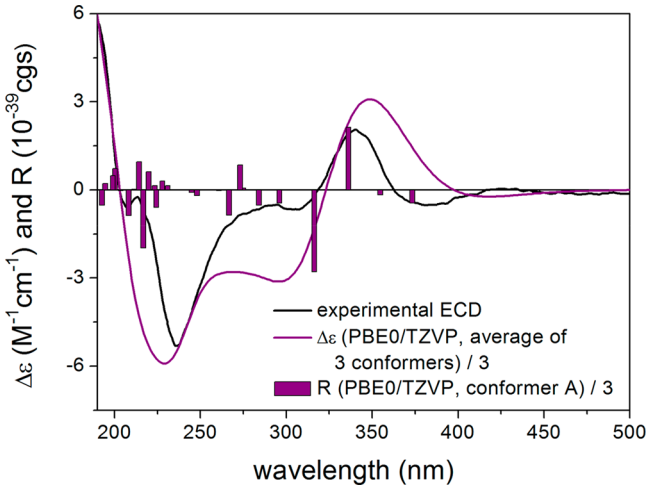

Figure 4. Experimental ECD spectrum of **1a** in MeCN (black line) compared with the calculated PBE0/TZVP PCM/MeCN spectrum of (1*R*,8a*R*)-**1** (purple line). Level of DFT optimization: ωB97X/TZVP PCM/MeCN. Bars represent the rotational strengths of conformer A.

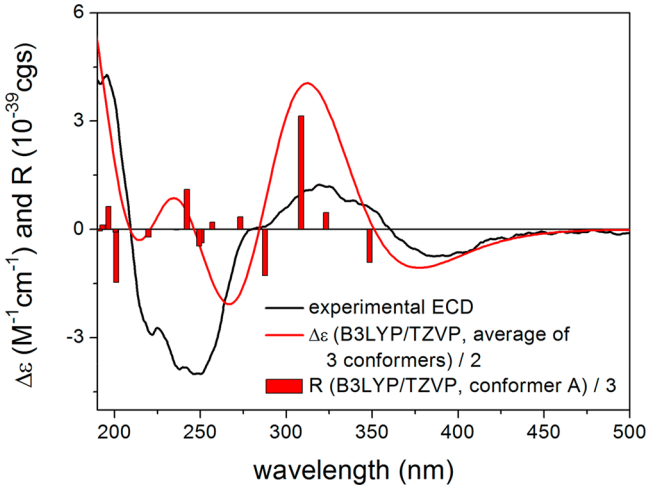

Figure 5. Experimental ECD spectrum of **1b** in MeCN (black line) compared with the calculated B3LYP/TZVP PCM/MeCN spectrum of (1*R*,8a*S*)-**1** (red line). Level of DFT optimization: ωB97X/TZVP PCM/MeCN. Bars represent the rotational strengths of conformer A.

and C-7 (δ_C 134.1), respectively. Methoxy groups attached at C-4a and C-8a were positioned by means of the HMBC interactions between δ_H 3.04 (CH_3O-4a) and δ_C 73.1 (C-4a), and between δ_H 2.72 (CH_3O-8a) and δ_C 75.1 (C-8a). The vinylic system was connected to C-8 via cross peaks between δ_H 5.63, dd, 5.78, dd and δ_C 150.2.

All NMR characteristics of compound **2b** were similar to compound **2a**, indicating that they are diastereomers. The main differences between **2b** and **2a** were found between the ^{13}C NMR chemical shifts of C-4a and 8a and adjacent carbons, suggesting that **2b** and **2a** differ in the configurations of C-4a and 8a.

In the case of racemic compound **3**, the signals of four *o*-coupled aromatic protons [(δ_H 6.30, d and 9.06, d (H-3−H-4), δ_H 8.19, d and 7.60, d (H-9−H-10)], two methyls (δ_H 1.58, s and 2.42, s), a vinyl group (δ_H 6.98, dd, 5.82, dd and 5.38, dd, H-13 and H_2-14), and two methoxy groups (δ_H 3.08, s, and 3.79, s) were detected in the ^{1}H NMR data (Table 1). The differences between juncuenin B and compound **3** involved the

https://dx.doi.org/10.1021/acs.jnatprod.0c00499
J. Nat. Prod. 2020, 83, 3250−3261

presence of an aromatic ring B, the oxidation of the phenolic group at C-2 to a carbonyl moiety (δ_C 202.4), and the addition of methoxy groups at C-1 and C-5.

The ^{1}H NMR spectrum of the racemic mixture of **4a** and **4b** differ from juncuenin B in the presence of a methoxy group (δ_H 2.85) (Table 1) and the carbonyl group at ring C. In the JMOD spectrum 19 carbon signals were observed (Table 2). The methoxy group was located at C-8a, as the aforementioned CH_3O proton signal showed HMBC correlation with the carbon signal resonating at δ_C 73.8. Following the NMR studies the enantiomers **4a** and **4b** were separated on a Lux amylose-1 chiral-phase HPLC column [t_R = 5.5 min (**4a**) and 10.3 min (**4b**)].

The 1D NMR data of compound **5** were found to be similar to those of **2a** and **2b**, except for the presence of two ethoxy groups in the molecule [δ_H 2.96, dq/3.29, dq, 2.76 dq/3.08, dq (CH_2) and 0.80, t/1.11, t (CH_3); δ_C 59.0/60.2 (CH_2), 14.7/15.8 (CH_3)]. Relevant HMBC interactions suggested the side chains to be attached to the phenanthrene skeleton at C-4a and C-8a (Tables 1 and 2).

Compounds **6a** and **6b** were obtained as racemic diastereomers. The difference between compounds **1a**−**d** and compounds **6a** and **6b** involved the replacement of the C-1 and C-8a methoxy groups with ethoxy substituents (Tables 1 and 2).

Compounds **7a** and **7b** differ from compounds **4a** and **4b** in the presence of an ethoxy group [δ_H 2.92, m, 3.11, m (CH_2), 0.86, t (CH_3); δ_C 59.5 (CH_2), 15.4 (CH_3)] at C-8a instead of a methoxy group (Tables 1 and 2). Compounds **7a** and **7b**, similar to **1a**−**d** and **4**−**6**, also contain a carbonyl moiety at C-6 (δ_C 186.6). Following the NMR analysis, the enantiomers **7a** and **7b** were separated by HPLC on a Lux amylose-1 chiral-phase column [t_R = 4.7 min (**7a**) and 9.1 min (**7b**)] and mirror-image ECD spectra were recorded (Figure 6).

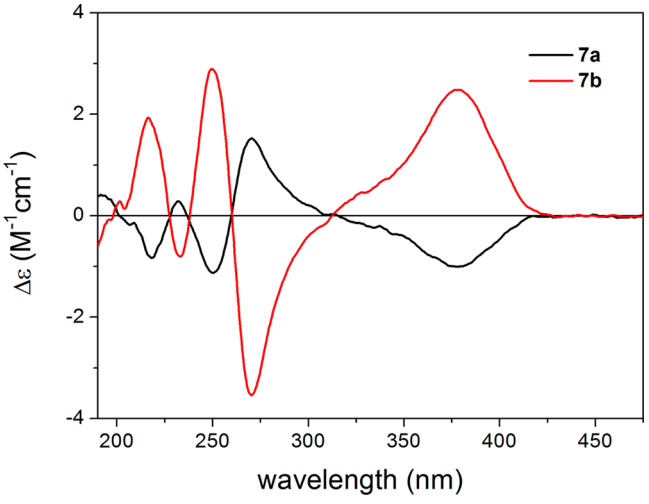

Figure 6. Experimental ECD spectra of **7a** and **7b** in MeCN.

For the configurational assignments of **7a** and **7b**, the above-mentioned TDDFT-ECD protocol was applied to (*R*)-**7** and also on the truncated methoxy model compound (*R*)-**4**.

DFT reoptimization of the initial six MMFF conformers of both (*R*)-**4** and (*R*)-**7** yielded six conformers above 1% population indicating that the ethoxy group does not have considerable freedom (Figure S64, Supporting Information). The Boltzmann-weighted ECD spectra of both sets of conformers reproduced well the experimental ECD spectrum of the first-eluting enantiomer **7a** (Figure 7 and Figure S37, Supporting Information). Consequently, the absolute configurations of **7a** and **4a**, which were separated under the same conditions, could be elucidated as (*R*) and that of the second-eluting **7b** and **4b** as (*S*).

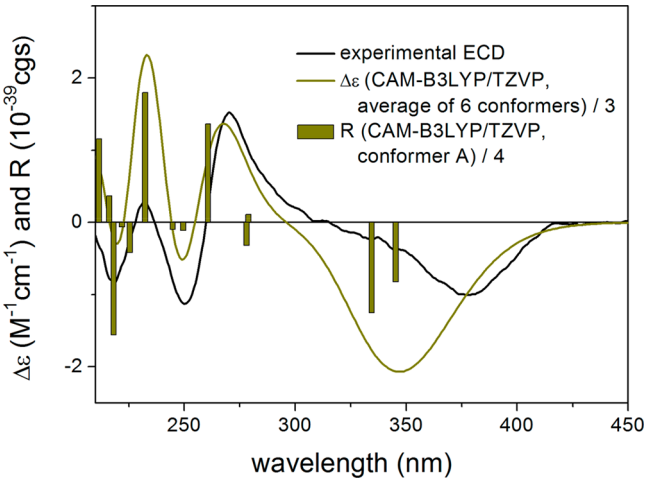

Figure 7. Experimental ECD spectrum of **7a** in MeCN (black line) compared with the calculated CAM-B3LYP/TZVP PCM/MeCN spectrum of (*R*)-**7a** (olive line). Level of DFT optimization: ωB97X/TZVP PCM/MeCN. Bars represent the rotational strengths of conformer A.

Interestingly, racemic compound **8** is the only one in which ring C is unchanged compared to the starting material, juncuenin B. An ethoxy group [δ_H 3.00, dq, 3.28, dq (CH_2), 1.20, t (CH_3); δ_C 62.2 (CH_2), 15.8 (CH_3)] is attached at C-1, and the phenolic group at C-2 of juncuenin B was oxidized to a carbonyl moiety (δ_C 202.9). Moreover, **8** is an unsaturated compound containing a $\Delta^{9,10}$ double bond (δ_H 8.15, d and 7.61, d, H-9−H-10).

Compound **9** is a unique derivative because an ethoxy group [δ_H 3.13, dq, 3.26, dq (CH_2), 1.17, t (CH_3); δ_C 61.6 (CH_2), 15.6 (CH_3)] is attached to the phenanthrene skeleton at C-7, as suggested by spectroscopic data evidence. The HMBC correlation of H_3-12 (δ_H 1.49) with the oxygen-bearing C-7 at δ_C 82.1, as well as the relevant cross peaks H-5/C-7, H-13/C-7, H-5/C-8a, and H-13/C-8a indicated the presence of a $\Delta^{8,8a}$ double bond instead of a $\Delta^{7,8}$ olefinic bond, to support the above conclusion.

In the case of compound **10**, it was apparent from the 1D NMR spectra that three *n*-butoxy groups are connected to the phenanthrene skeleton. Both the phenolic substituents of juncuenin B were oxidized to carbonyl groups, and a $\Delta^{9,10}$ double bond was also formed. The location of the methyl, vinyl, and *n*-butoxy groups were determined by their diagnostic HMBC correlations. Three-bond heteronuclear interactions of C-1 (δ_C 81.9) with the oxymethylene protons at δ_H 2.92, m, and of the deshielded C-5 (δ_C 94.6) with two additional oxymethylenes at δ_H 3.14, m, and 3.54, m confirmed the positions of the *n*-butoxy groups at C-1 and C-5, respectively.

The ^{1}H NMR spectrum of the racemic compound **11** displayed signals attributable to an *n*-butoxy moiety [δ_H 2.83, m, 3.07, m (CH_2), 1.13−1.23, m (CH_2) 0.86−1.03, m (CH_2), and 0.62, t (CH_3); δ_C 63.5 (CH_2), 31.9 (CH_2), 19.1 (CH_2), and 13.7 (CH_3)]. Since the oxidative transformation was

https://dx.doi.org/10.1021/acs.jnatprod.0c00499
J. Nat. Prod. 2020, 83, 3250−3261

Table 3. IC_{50} Values (μM, Mean ± SEM) of the Diastereomeric and/or Racemic Mixtures[a]

	calculated IC_{50} values (μM ± SEM)				
compound	MCF-7	HeLa	C33A	A2780	NIH/3T3
juncuenin B	–	2.9 ± 0.5[b]	–	7.3 ± 1.3[b]	>30
1a−1d	–	–	6.7 ± 0.5	7.7 ± 1.0	17.7 ± 0.7
4a+4b	6.5 ± 1.1	1.9 ± 0.4	7.0 ± 1.8	9.1 ± 0.5	14.9 ± 3.7
7a+7b	6.2 ± 0.2	5.4 ± 0.1	6.1 ± 0.4	5.9 ± 1.1	>30
cisplatin	5.8	–	1.8	1.3[b]	2.7

[a]Compounds **2a**, **2b**, **3**, **5**, **6b**, **8**, **9**, and **10** were found to be inactive or moderately active (Table S1, Supporting Information). Determinations were performed using an MTT assay by treating the cells with compounds (0.1−30 μM) for 72 h. Data are based on two independent experiments. [b]IC_{50} value from literature.[10]

Table 4. IC_{50} Values of the Enantiopure Compounds 1a−1d, 4a, 4b, 7a, and 7b[a]

	Calculated IC_{50} values (μM ± SEM)					
compound	MCF-7	T47D	HeLa	C33A	A2780	NIH/3T3
(1*R*,8a*S*)-**1b**	–	–	–	–	9.0 ± 1.0	>30
(1*S*,8a*R*)-**1c**	–	–	–	5.3 ± 0.9	7.7 ± 0.6	21.6 ± 0.4
(8a*R*)-**4a**	6.2 ± 1.6	–	0.9 ± 0.4	5.3 ± 0.6	8.7 ± 0.8	25.8 ± 4.6
(8a*R*)-**7a**	–	8.8 ± 1.1	3.7 ± 0.9	4.9 ± 0.3	2.8 ± 0.3	>30
cisplatin	5.8	9.8[b]	–[b]	1.8	1.3[b]	2.7

[a]Determinations were performed using an MTT assay by treating the cells with compounds (0.1−30 μM) for 72 h. Data are based on two independent experiments. [b]IC_{50} value from literature.[10]

performed in a reaction medium containing *n*-BuOH as solvent, and the aromatic A-ring and HO-2 remained intact during the reaction, it was anticipated that the *n*-butoxy chain is situated at C-8a. This presumption was corroborated by a strong HMBC cross peak between the oxymethylene protons and C-8a.

The antiproliferative assays of the products were carried out by a standard MTT method on human breast (MCF-7, T47D), cervical (HeLa, SiHa, C33A), and ovarian (A2780) cancer cells, and NIH/3T3 mouse embryonic fibroblast cell lines. In the first step, the diastereomeric and racemic mixtures **1**−**11** and the starting compound, juncuenin B, were tested to obtain information about their antiproliferative activity. Among the tested samples, compounds **1a**−**d**, **4a**+**4b**, **6a**, **7a**+**7b**, and **11** exhibited significant tumor cell proliferation inhibitory activities with IC_{50} values close to that of juncuenin B (Table 3, and Tables S2 and S3, Supporting Information). The IC_{50} value of juncuenin B on MCF-7 cell line (11.7 μM) was determined for the first time. Similar to the structural points of view, it is evident that compounds without a *p*-quinol ring (**3**, **8**, **9**, and **10**) and compounds with two *p*-quinol moieties (**2a**, **2b**, **5**) did not exert antiproliferative activity. Compounds substituted at C-4a with an alkoxy group were also inactive. Compounds **1a**−**d** (IC_{50}s 11.6 μM on MCF-7, 15.0 μM on T47D, 15.6 μM on HeLa, 20.0 μM on SiHa, 6.7 μM on C33A, and 7.7 μM on A2780, respectively), **4a**+**4b** (IC_{50}s 6.5 μM on MCF-7, 1.9 μM on HeLa, 7.0 μM on C33A, and 9.1 μM on A2780, respectively), and **7a**+**7b** (IC_{50}s 6.2 μM on MCF-7, 16.9 μM on T47D, 5.4 μM on HeLa, 6.1 μM on C33A and 5.9 μM on A2780, respectively) with the highest activity were selected for further studies.

In the second step, the enantiomerically pure compounds (**1a**, **1b**, **1c**, **1d**, **4a**, **4b**, and **7b**) were evaluated for their antiproliferative activity against the same cell lines (Table 4). Among these compounds, the highest activities were recorded for **1c**, **4a**, and **7a**, reaching or exceeding that of the positive control cisplatin against HeLa and/or T47D cell lines. (*R*)-**7a** was found to be the most promising compound with substantial antiproliferative effects against all tested cell lines except for SiHa, but it was inactive against the nontumoral NIH/3T3 cells.

Compounds **4a**, **4b**, **7a**, **7b**, and **11** contain a nonoxidized A ring and a C-ring comprising a *p*-quinol alkyl ether moiety. Moreover, **4a** and **4b** are substituted with a methoxy-, **7a**, and **7b** with an ethoxy-, and **11** with an *n*-butoxy group at C-8a, respectively. In the case of these compounds, the effect of the length of the ether chain at C-8a is undefined: on the T47D, HeLa, C33A, and A2780 cell lines, compound **7a** with an ethoxy group, showed the highest inhibition, while its enantiomer (**7b**) had no activity. On the HeLa cell line, the antiproliferative activity was inversely proportional to the chain length of the alkoxy groups (IC_{50} values **11** > **7a** > **4a**). Compounds **4a** and **7a** showed an antiproliferative effect on HeLa, C33A, MCF-7, and A2780 cells, which was comparable to or stronger than that of juncuenin B, while their stereoisomers **4b** and **7b** had no relevant influence on the cell proliferation, indicating that (8a*R*) is the preferred absolute configuration of these compounds. Regarding the pure enantiomers **1a**−**d**, the (1*S*,8a*R*)-configuration (**1c**) was the most beneficial for the antiproliferative effect. The activities of (1*S*,8a*R*)-**1c**, (*R*)-**4a**, and (*R*)-**7a** suggest the preference of the (*R*) configuration for the antiproliferative activity. Since **1a** is less active than **1c**, the (1*S*) configuration seems to be also essential in the case of quinoidal compounds.

It is worth mentioning that several of the semisynthetic compounds demonstrated an altered cell line specificity as compared to their parent compound, juncuenin B. For example, while juncuenin B exerted approximately 2.5-fold stronger activity on MCF-7 than on T47D cells, a similar rate of selectivity in the opposite direction was observed for the enantiopure compound **7a**. While both of these cell lines are estrogen receptor α positive and therefore estrogen-dependent, they show critical differences in their bioenergetic properties,[21] as well as in apoptotic events including the activation of different caspases and mitochondrial changes.[22] This selectivity inversion suggests that compounds obtained from juncuenin B

https://dx.doi.org/10.1021/acs.jnatprod.0c00499
J. Nat. Prod. 2020, 83, 3250−3261

were not only more potent than the starting material, but also these compounds likely act on different biochemical targets. Further studies are necessary for the clarification of these targets, but chemical analogies from our previous work suggest the involvement of ATR-dependent signaling at least to some extent.[12,13]

In conclusion, oxidation of juncuenin B with hypervalent iodine reagents under different conditions resulted in the identification of phenanthrene derivatives substituted with hydroxy, methyl, methoxy, vinyl, ethoxy and *n*-butoxy groups. The majority of the components contain a substituted *p*-quinol ring. All compounds are reported here for the first time. Several compounds showed promising antiproliferative activities, and based on their structural analogy, structure−activity relationships were deduced. No significant activities were observed either for compounds without a substituted *p*-quinol ring (**3**, **8**, **9**, and **11**), or for those containing two such rings (**2a**, **2b**, and **5**). However, derivatives containing one substituted *p*-quinol ring showed promising antiproliferative activities against different human cancer cell lines, and this was observed for compounds with an *o*-alkoxy-quinone moiety (**1a**−**d**, **6a**) and for those with an intact A ring (**4a**, **7a**, and **11**). Clarifying the mechanism of action for these compounds requires further studies.

In the current work, similar structural elements were introduced in juncuenin B as present in denbinobin and calanquinone. The aromatic ring oxidations of juncuenin B afforded quinols which were found to be bioactive to the same degree as the lead compounds denbinobin and calanquinone. The starting compound juncuenin B can be readily isolated in a good yield (0.043% w/w) from *Juncus inflexus* root. There is a strong rationale for further development of oxidized derivatives of juncuenin B in the future.

EXPERIMENTAL SECTION

General Experimental Procedures. NMR spectra were recorded in methanol-d_4 and $CDCl_3$ on a Bruker Avance DRX 500 spectrometer at 500 MHz (^{1}H) and 125 MHz (^{13}C). The signals of the deuterated solvents were used as references. The chemical shift values (δ) are given in ppm and coupling constants in Hz. 2D experiments were performed with standard Bruker software. In the ^{1}H−^{1}H COSY, HSQC, and HMBC experiments, gradient-enhanced versions were applied. The HRMS data were acquired on a Thermo Scientific Q-Exactive Plus Orbitrap mass spectrometer equipped with ESI ion source in positive ionization mode. The data were acquired and processed with MassLynx software. ECD and UV spectra were recorded on a J-810 spectropolarimeter.

In the reaction processes [bis(trifluoroacetoxy)iodo]benzene (PIFA) and (diacetoxyiodo)benzene (PIDA) were used as oxidizing agents (Sigma-Aldrich, Stockholm, Sweden). To reaction progress and separation steps were monitored by TLC on Kieselgel 60F_{254} silica plates obtained from Merck (Merck, Darmstadt, Germany), and examined under UV light at 254 and 366 nm. Solid phase extraction (SPE) was carried out on silica gel (Kieselgel 60 GF_{254}, 15 μm, Merck). MPLC was performed with a Combi Flash Rf$^+$ Lumen instrument (Teledyne Isco). All solvents used for MPLC were of at least analytical grade (VWR Ltd., Szeged, Hungary). Both the reaction mixtures and processed fractions were investigated by HPLC on a Jasco instrument equipped with an MD-2010 Plus PDA detector (Jasco Analytical Instruments, Japan) in a detection range of 210−400 nm, with an Agilent Eclipse XDB C_8 column (4.6 × 150 mm, 5 μm) (Agilent Technologies, Inc., USA). MeCN−H_2O solvent system was used as eluent. The final purification steps were carried out by using HPLC with an Agilent Eclipse XDB C_8 (9.4 × 250 mm, 5 μm) (Agilent Technologies, Inc., USA) equipment, and MeCN−H_2O mixture as the mobile phase. Enantiomers were separated by using a Lux amylose-1 column (250 × 21.2 mm) (Phenomenex, USA), using a cyclohexane−isopropanol solvent system as mobile phase. The HPLC system for semipreparative separations comprised of a Waters 600 controller, Waters 600 pump, and Waters 2998 photodiode array detector. The data were acquired and processed with the Empower software.

The antiproliferative activity and tumor selectivity of the compounds were measured by standard MTT assays. Tumor cell lines MCF-7, T47D, HeLa, A2780, and noncancerous NIH/3T3 were provided by European Collection of Authenticated Cell Cultures (ECACC, Salisbury, UK); cell lines SiHa and C33A by LGC Standards GmbH (Wesel, Germany). All chemicals and materials used for the antiproliferative assays were purchased from Sigma Aldrich Ltd. (Budapest, Hungary).

Juncuenin B. Juncuenin B was isolated previously from the MeOH extract of *Juncus inflexus* roots by chromatographic methods (VLC on silica gel, and gel chromatography on Sephadex LH-20). *J. inflexus* is a good source of this compound as approximately 1.5 g was isolated (0.043% w/w) in crystalline form from 3.5 kg dried plant material.[23]

Synthesis and Purification Process. In reaction I, 50 mg juncuenin B was dissolved in MeCN−MeOH (9:1) at a concentration of 1 mg/mL, and stirred with 2 equiv of PIFA (161.2 mg) for 30 min at 0 °C. After drying under nitrogen gas, SPE was applied to absorb the remaining oxidizing agent and the possibly decomposed compounds. Thereafter, the reaction mixture was fractionated by MPLC with *n*-hexane−EtOAc gradient solvent system to obtain five fractions (I/1−5). From fraction I/1 compounds **1a**−**d** (1.00 mg, 2% each) were isolated by RP-HPLC using MeCN−H_2O (1:1) as eluent (3 mL/min flow rate). Fraction I/2 was purified by RP-HPLC, MeCN−H_2O (3:2) (3 mL/min flow rate) was applied as eluent to gain compounds **2a** (0.88 mg) and **2b** (0.75 mg).

For process reaction II, 100 mg juncuenin B was dissolved in anhydrous MeOH at a concentration of 1 mg/mL, and stirred with 2 equiv of PIFA (322.32 mg) for 30 min at room temperature. After evaporating the solvent under reduced pressure, SPE was applied to absorb the remaining oxidizing agents and the possibly decomposed compounds. The mixture was fractionated by MPLC with *n*-hexane−EtOAc gradient solvent system to obtain four fractions. Fraction II/1, after being chromatographed by RP-HPLC using MeCN−H_2O (1:1) (flow rate 3 mL/min) as mobile phase, compounds **1a**−**d** (2.00 mg) and **5** (3.8 mg) were obtained. Fractions II/2 and II/3 were separated under the same conditions as II/1. From fraction II/2 **1a**−**d** (1.00 mg) and **3** (1.8 mg); from II/3 compounds **1a**−**d** (3.00 mg) and **4a**,**b** (2.00 mg) were isolated.

In the case of reaction III, 100 mg juncuenin B was dissolved in anhydrous EtOH at a concentration of 1 mg/mL, and stirred with 2 equiv of PIFA (322.32 mg) for 30 min at room temperature. After evaporating the solvent under reduced pressure, SPE was applied to remove the remaining oxidizing agents and decomposed compounds. The mixture was fractionated by MPLC with a gradient solvent system of *n*-hexane−EtOAc to obtain 10 fractions (III/1−10). Fraction III/1 afforded compound **5** (1.6 mg) after purification by HPLC with MeCN−H_2O (1:1) as mobile phase (flow rate 3 mL/min). Fraction III/2 was rechromatographed by RP-HPLC, using an MeCN−H_2O gradient system (flow rate 3 mL/min) as eluent to yield compounds **6a** (3.0 mg) and **6b** (1.85 mg). Fraction III/4 was found to be pure and gave compounds **7a**,**b** (13.0 mg). Fraction III/6 was subjected to HPLC using MeCN−H_2O (1:1) (flow rate 3 mL/min) as mobile phase and afforded compounds **7a**,**b** (4.4 mg, 4.4%) and **8** (2.1 mg). Fraction III/7 was purified by RP-HPLC with MeCN−H_2O (1:1) as eluent to give compound **9** (1.80 mg).

In reaction IV, 50 mg juncuenin B was dissolved in *n*-BuOH at a concentration of 1 mg/mL, and stirred with 2 equiv of PIFA (161,15 mg) for 30 min at room temperature. After evaporating the solvent under reduced pressure, prepurification with SPE was performed and the resulting mixture was fractionated by MPLC with an *n*-hexane−EtOAc gradient system to afford six fractions (IV/1−6). From fraction IV/1 compound **10** (1.80 mg) was isolated.

https://dx.doi.org/10.1021/acs.jnatprod.0c00499
J. Nat. Prod. 2020, 83, 3250−3261

For reaction V, 100 mg juncuenin B was dissolved in *n*-BuOH at a concentration of 1 mg/mL, and stirred with 2 equiv of PIDA (242 mg) for 30 min at room temperature. The solvent was evaporated under reduced pressure, and then SPE was used to absorb the remaining oxidizing agents and other impurities. The mixture was fractionated by MPLC with an *n*-hexane−EtOAc gradient solvent system to afford four fractions (V/1−4). Fraction V/2 was subjected to HPLC, eluting with MeCN−H_2O (3:2) (flow rate 3 mL/min) as mobile phase to give compound **11** (5.5 mg).

Separation of Enantiomers. Racemic mixtures, which had high antiproliferative activity, were separated on a Lux amylose-1 chiral-phase column in order to compare the antiproliferative activity of the pure enantiomers. For the separation of compounds **1a−d**, cyclohexane−isopropanol (95:5) and for compounds **4a+b** and **7a+b** cyclohexane−isopropanol (8:2) solvent systems (15 mL/min) were used as eluent.

*(1R,8aR)-**1a***. Pale yellow solid; $[\alpha]_D$: −17 (*c* 0.1, $CHCl_3$); HRESIMS *m/z* 327.1596 $[M + H]^+$ (calcd for $C_{20}H_{23}O_4$, 327.1592); UV (MeCN) λ_{max} (log ε) 295sh (3.53), 220sh (3.95) nm; ECD {CH_3CN, λ_{max} [nm] ($\Delta\varepsilon$)}, *c* 5.97 × 10^{-4} M: 382 (−0.52), 341 (+2.05), 304sh (−0.67), 236 (−5.31), 207sh (−0.59); ^1H and ^{13}C NMR data, see Tables 1 and 2; HPLC: Lux amylose-1 chiral-phase column, cyclohexane−isopropanol (95:5) solvent system, flow rate 15 mL/min, t_R = 13.6 min.

*(1S,8aR)-**1b***. $[\alpha]_D$: −26 (*c* 0.1, $CHCl_3$); UV (MeCN) λ_{max} (log ε) 294sh (3.57), 221sh (4.01) nm; ECD {CH_3CN, λ_{max} [nm] ($\Delta\varepsilon$)}, *c* 4.90 × 10^{-4} M: 393 (−0.74), 338sh (+0.80), 319 (+1.24), 246 (−4.01), 222sh (−2.92), 196 (+4.29); ^1H and ^{13}C NMR data, see Tables 1 and 2. HPLC: Lux amylose-1 chiral-phase column, cyclohexane−isopropanol (95:5) solvent system, flow rate 15 mL/min, t_R = 17.4 min.

*(1S,8aS)-**1c***. $[\alpha]_D$: +26 (*c* 0.1, $CHCl_3$); UV (MeCN) λ_{max} (log ε) 294sh (3.57), 221sh (4.01) nm; ECD {CH_3CN, λ_{max} [nm] ($\Delta\varepsilon$)}, *c* 5.31 × 10^{-4} M: 390 (+0.49), 336sh (−0.81), 317 (−1.14), 253sh (+2.87), 237 (+3.81), 218sh (+2.27), 194 (−3.41); ^1H and ^{13}C NMR data, see Tables 1 and 2. HPLC: Lux amylose-1 chiral-phase column, cyclohexane−isopropanol (95:5) solvent system, flow rate 15 mL/min, t_R = 21.6 min.

*(1R,8aS)-**1d***. $[\alpha]_D$: +23 (*c*, 0.1, $CHCl_3$); UV (MeCN) λ_{max} (log ε) 295sh (3.53), 220sh (3.95) nm; ECD {CH_3CN, λ_{max} [nm] ($\Delta\varepsilon$)}, *c* 5.36 × 10^{-4} M: 384 (+0.39), 338 (−1.52), 303sh (+0.43), 236 (+3.79), 209sh (+0.49); ^1H and ^{13}C NMR data, see Tables 1 and 2. HPLC: Lux amylose-1 chiral-phase column, cyclohexane−isopropanol (95:5) solvent system, flow rate 15 mL/min, t_R = 23.6 min.

*Ent-**2a***. Pale yellow solid; HRESIMS *m/z* 327.1598 $[M + H]^+$ (calcd for $C_{20}H_{23}O_4$, 327.1591); ^1H and ^{13}C NMR data, see Tables 1 and 2.

*Ent-**2b***. Pale yellow solid; HRESIMS see ent-**2a**; ^1H and ^{13}C NMR data, see Tables 1 and 2.

*Rac-**3***. White solid, HRESIMS *m/z* 325.1435 $[M + H]^+$ (calcd for $C_{20}H_{21}O_4$, 325.1434); ^1H and ^{13}C NMR data, see Tables 1 and 2.

*(8aR)-**4a*** + *(8aS)-**4b***. Pale yellow solid; HRESIMS *m/z* 297.1488 $[M + H]^+$ (calcd for $C_{19}H_{21}O_3$ 297.1485); ^1H and ^{13}C NMR data, see Tables 1 and 2; HPLC: Lux amylose-1 chiral column, cyclohexane−isopropanol (8:2) solvent system, flow rate 50 mL/min, t_R = 5.5 min (**4a**) and 10.3 min (**4b**).

*(4aR,S;8aR,S)-**5***. Pale yellow solid; HRESIMS *m/z* 355.1913 $[M + H]^+$ (calcd for $C_{22}H_{27}O_4$ 355.1904; ^1H and ^{13}C NMR data, see Tables 1 and 2.

*Ent-**6a***. White solid; ^1H and ^{13}C NMR data, see Tables 1 and 2; HRESIMS *m/z* 355.1903 $[M + H]^+$ (calcd for $C_{22}H_{27}O_4$ 355.1904).

*Ent-**6b***. White solid; ^1H and ^{13}C NMR data, see Tables 1 and 2; HRESIMS see ent-**6a**.

*(8aR)-**7a***. Pale yellow solid; $[\alpha]_D$: −124 (*c*, 0.1, $CHCl_3$); HRESIMS *m/z* 355.1915 (calcd for $C_{20}H_{23}O_3$ 355.1909); ECD {CH_3CN, λ_{max} [nm] ($\Delta\varepsilon$)}, *c* 5.07 × 10^{-4} M: 378 (−1.01), 333sh (−0.23), 302sh (+0.19), 271 (+1.52), 250 (−1.13), 232 (+0.28), 218 (−0.84); ^1H and ^{13}C NMR data, see Tables 1 and 2; HPLC: Lux amylose-1 chiral-phase column, cyclohexane−isopropanol (8:2) solvent system, flow rate 15 mL/min, t_R = 4.7 min.

*(8aS)-**7b***. Pale yellow solid; $[\alpha]_D$: +148 (*c*, 0.1, $CHCl_3$); HRESIMS see (8a*R*)-**7a**; ECD {CH_3CN, λ_{max} [nm] ($\Delta\varepsilon$)}, *c* 4.91 × 10^{-4} M: 379 (+2.48), 334sh (+0.55), 271 (−3.54), 250 (+2.89), 233 (−0.81), 217 (+1.94); ^1H and ^{13}C NMR data, see Tables 1 and 2. HPLC: Lux amylose-1 chiral-phase column, cyclohexane−isopropanol (8:2) solvent system, flow rate 15 mL/min, t_R = 9.1 min.

*Rac-**8***. White solid; HRESIMS *m/z* 309.1491 $[M + H]^+$ (calcd for $C_{20}H_{21}O_3$ 309.1485); ^1H and ^{13}C NMR data, see Tables 1 and 2.

*Rac-**9***. White solid; HRESIMS *m/z* 311.1646 $[M + H]^+$ (calcd for $C_{20}H_{23}O_3$ 311.1642); ^1H and ^{13}C NMR data, see Tables 1 and 2.

*Rac-**10***. Light brown solid; HRESIMS *m/z* 481.2948 $[M + H]^+$ (calcd for $C_{30}H_{41}O_5$ 481.2949); ^1H and ^{13}C NMR data, see Tables 1 and 2.

*Rac-**11***. Light brown solid; HRESIMS *m/z* 339.1959 $[M + H]^+$ (calcd for $C_{22}H_{27}O_3$ 339.1955); ^1H and ^{13}C NMR data, see Tables 1 and 2.

Computational Methods. Mixed torsional/low-mode conformational searches were carried out by means of the Macromodel 10.8.011 software using the MMFF with an implicit solvent model for $CHCl_3$ applying a 21 kJ/mol energy window.[24] Geometry reoptimizations of the resultant conformers (ωB97X/TZVP with PCM solvent model for MeCN) and TDDFT ECD calculations were performed with Gaussian 09.[25] For ECD using various functionals (B3LYP, BH&HLYP, CAM-B3LYP, PBE0) and the TZVP basis set with the same solvent model as in the preceding DFT optimization step. ECD spectra were generated as the sum of Gaussians with 3000 cm^{-1} half-height widths, using dipole-velocity computed rotational strengths.[26] Boltzmann distributions were estimated from the ωB97X energies. The MOLEKEL program was used for visualization of the results.[27]

Antiproliferative (MTT) Assay. Growth-inhibition properties of racemates and pure enantiomer compounds were determined by standard MTT assays on six human malignant gynecological cell lines (MCF-7, T47D, HeLa, SiHa, C33A, A2780). To investigate tumor selectivity, the MTT assay was repeated on mouse embryonic fibroblast cells (NIH/3T3) under the same conditions. All cell lines were maintained in minimal essential medium (MEM) supplemented with 10% fetal bovine serum, 1% nonessential amino acids, and 1% penicillin−streptomycin−amphotericin B mixture, and were stored in humidified air containing 5% CO_2 at 37 °C. All cell types were seeded into 96−well plates at a density of 5000 with the exception of C33a, which was seeded at a density of 10 000 and treated by increasing concentrations (0.1−30 μM) of the compounds for 72 h under cell culturing conditions. After the incubation, 5 mg/mL MTT [3-(4,5-dimethylthiazol-2-yl)-2,5-diphenyltetrazolium bromide] solution was added to samples for 4 h and precipitated blue formazan crystals were dissolved in DMSO. Absorbance values of the samples were measured at 545 nm using a microplate reader (Stat Fax-2100, Awareness Technologies Inc., Palm City, FL, USA) and untreated cells were used as control. Normalized sigmoidal dose−response curves were fitted to the determined data and the IC_{50} values were calculated by GraphPad Prism 5.01 (GraphPad Software, San Diego, CA, USA). Cisplatin (Ebewe Pharma GmbH, Unterach, Austria) was used as a reference agent in the same concentration range.

■ ASSOCIATED CONTENT

Supporting Information

The Supporting Information is available free of charge at https://pubs.acs.org/doi/10.1021/acs.jnatprod.0c00499.

1D and 2D NMR spectra of compounds **1**−**11** and ECD spectra of compounds **1**, **4**, and **7** (PDF)

■ AUTHOR INFORMATION

Corresponding Authors

Attila Hunyadi − *Department of Pharmacognosy, Interdisciplinary Excellence Centre, University of Szeged,*

https://dx.doi.org/10.1021/acs.jnatprod.0c00499
J. Nat. Prod. 2020, 83, 3250−3261

6720 Szeged, Hungary; Phone: +36-62-546456; Email: hunyadi.a@pharm.u-szeged.hu

Andrea Vasas − *Department of Pharmacognosy, Interdisciplinary Excellence Centre, University of Szeged, 6720 Szeged, Hungary*; orcid.org/0000-0002-1818-7702; Phone: +36-62-546451; Email: vasasa@pharm.u-szeged.hu

Authors

Csaba Bús − *Department of Pharmacognosy, Interdisciplinary Excellence Centre, University of Szeged, 6720 Szeged, Hungary*

Ágnes Kulmány − *Department of Pharmacodynamics and Biopharmacy, University of Szeged, 6720 Szeged, Hungary*

Norbert Kúsz − *Department of Pharmacognosy, Interdisciplinary Excellence Centre, University of Szeged, 6720 Szeged, Hungary*

Tímea Gonda − *Department of Pharmacognosy, Interdisciplinary Excellence Centre, University of Szeged, 6720 Szeged, Hungary*

István Zupkó − *Department of Pharmacodynamics and Biopharmacy, University of Szeged, 6720 Szeged, Hungary*

Attila Mándi − *Department of Organic Chemistry, University of Debrecen, 4032 Debrecen, Hungary*; orcid.org/0000-0002-7867-7084

Tibor Kurtán − *Department of Organic Chemistry, University of Debrecen, 4032 Debrecen, Hungary*; orcid.org/0000-0002-8831-8499

Barbara Tóth − *Department of Pharmacognosy, Interdisciplinary Excellence Centre, University of Szeged, 6720 Szeged, Hungary*

Judit Hohmann − *Department of Pharmacognosy, Interdisciplinary Excellence Centre, University of Szeged, 6720 Szeged, Hungary*; orcid.org/0000-0002-2887-6392

Complete contact information is available at: https://pubs.acs.org/10.1021/acs.jnatprod.0c00499

Author Contributions

‖Csaba Bús and Ágnes Kulmány are co-first authors.

Notes

The authors declare no competing financial interest.

■ ACKNOWLEDGMENTS

Financial support for this research was provided by the Economic Development and Innovation Operative Program GINOP-2.3.2-15-2016-00012, the UNKP-18-3 and UNKP-19-3-SZTE-169 New National Excellence Program of the Ministry of Human Capacities, the 20391-3/2018/FEKUSTRAT, and the National Research, Development and Innovation Office, Hungary (NKFIH; K128963, K119770, and K120181). A.M. was supported by the Janos Bolyai Research Scholarship of the Hungarian Academy of Sciences. The Governmental Information-Technology Development Agency (KIFU) is acknowledged for CPU time. The authors are grateful to Ibolya Hevérné Herke for her work on the preparative chiral-phase HPLC separations.

■ REFERENCES

(1) He, S.; Wu, B.; Pan, Y.; Jiang, L. *J. Org. Chem.* **2008**, *73*, 5233−5241.

(2) Tóth, B.; Hohmann, J.; Vasas, A. *J. Nat. Prod.* **2018**, *81*, 661−678.

(3) Kovács, A.; Vasas, A.; Hohmann, J. *Phytochemistry* **2008**, *69*, 1084−1110.

(4) Yang, K. C.; Uen, Y. H.; Suk, F. M.; Liang, Y. C.; Wang, Y. J.; Ho, Y. S.; Li, I. H.; Lin, S. Y. *World J. Gastroenterol.* **2005**, *11*, 3040−3045.

(5) Sanchez-Duffhues, G.; Calzado, M. A.; de Vinuesa, A. G.; Appendino, G.; Fiebich, B. L.; Loock, U.; Lefarth-Risse, A.; Krohn, K.; Muñoz, E. *Biochem. Pharmacol.* **2009**, *77*, 1401−1409.

(6) Lee, C. L.; Lin, Y. T.; Chang, F. R.; Chen, G. Y.; Backlund, A.; Yang, J. C.; Chen, S. L.; Wu, Y. C. *PLoS One* **2012**, *7*, e37897.

(7) Kuo, C. T.; Chen, B. C.; Yu, C. C.; Weng, C. M.; Hsu, M. J.; Chen, C. C.; Chen, M. C.; Teng, C. M.; Pan, S. L.; Bien, M. Y.; Shih, C. H.; Lin, C. H. *J. Biomed. Sci.* **2009**, *16*, 1−15.

(8) Liu, W.; Meng, M.; Zhang, B.; Du, L.; Pan, Y.; Yang, P.; Gu, Z.; Zhou, Q.; Cao, Z. *Toxicol. Appl. Pharmacol.* **2015**, *287*, 98−110.

(9) Zhang, B.; Han, H.; Fu, S.; Yang, P.; Gu, Z.; Zhou, Q.; Cao, Z. *Biochem. Pharmacol.* **2016**, *104*, 8−18.

(10) Kuo, C. Y.; Schelz, Z.; Tóth, B.; Vasas, A.; Ocsovszki, I.; Chang, F. R.; Hohmann, J.; Zupkó, I.; Wang, H. C. *Phytomedicine* **2019**, *58*, 152770.

(11) Hunyadi, A. *Med. Res. Rev.* **2019**, *39*, 2505.

(12) Fási, L.; Di Meo, F.; Kuo, C. Y.; Buric, S. S.; Martins, A.; Kúsz, N.; Béni, Z.; Dékány, M.; Balogh, G. T.; Pesic, M.; Wang, H. C.; Trouillas, P.; Hunyadi, A. *J. Med. Chem.* **2019**, *62*, 1657−1668.

(13) Wang, H. C.; Lee, A. Y.; Chou, W. C.; Wu, C. C.; Tseng, C. N.; Liu, K. Y.; Lin, W. L.; Chang, F. R.; Chuang, D. W.; Hunyadi, A.; Wu, Y. C. *Mol. Cancer Ther.* **2012**, *11*, 1443−1453.

(14) Lecona, E.; Fernandez-Capetillo, O. *Nat. Rev. Cancer* **2018**, *18*, 586−595.

(15) Kürti, L.; Herczegh, P.; Visy, J.; Simonyi, M.; Antus, S.; Pelter, A. *J. Chem. Soc., Perkin Trans. 1* **1999**, 379−380.

(16) Kita, Y.; Tohma, H.; Hatanaka, K.; Takada, T.; Fujita, S.; Mitoh, S.; Sakurai, H.; Oka, S. *J. Am. Chem. Soc.* **1994**, *116* (9), 3684−3691.

(17) (a) Superchi, S.; Scafato, P.; Gorecki, M.; Pescitelli, G. *Curr. Med. Chem.* **2018**, *25*, 287−320. (b) Mándi, A.; Kurtán, T. *Nat. Prod. Rep.* **2019**, *36*, 889−918.

(18) Chai, J. D.; Head-Gordon, M. *J. Chem. Phys.* **2008**, *128*, 084106.

(19) (a) Adamo, C.; Barone, V. *J. Chem. Phys.* **1998**, *108*, 664−675. (b) Kicsak, M.; Mandi, A.; Varga, S.; Herczeg, M.; Batta, G.; Benyei, A.; Borbas, A.; Herczegh, P. *Org. Biomol. Chem.* **2018**, *16*, 393−401.

(20) Pan, F.; El-Kashef, D. H.; Kalscheuer, R.; Müller, W. E. G.; Lee, J.; Feldbrügge, M.; Mándi, A.; Kurtán, T.; Liu, Z.; Wu, W.; Proksch, P. *Eur. J. Med. Chem.* **2020**, *191*, 112159.

(21) Radde, B. N.; Ivanova, M. M.; Mai, H. X.; Salabei, J. K.; Hill, B. G.; Klinge, C. M. *Biochem. J.* **2015**, *465*, 49−61.

(22) Mooney, L. M.; Al-Sakkaf, K. A.; Brown, B. L.; Dobson, P. R. M. *Br. J. Cancer* **2002**, *87*, 909−917.

(23) Tóth, B.; Liktor-Busa, E.; Kúsz, N.; Szappanos, Á; Mándi, A.; Kurtán, T.; Urbán, E.; Hohmann, J.; Chang, F. R.; Vasas, A. *J. Nat. Prod.* **2016**, *79*, 2814−2823.

(24) *MacroModel*; Schrödinger, LLC, 2015. http://www.schrodinger.com/MacroModel.

(25) Frisch, M. J.; Trucks, G. W.; Schlegel, H. B.; Scuseria, G. E.; Robb, M. A.; Cheeseman, J. R.; Scalmani, V.; Barone, G.; Mennucci, B.; Petersson, G. A.; Nakatsuji, H.; Caricato, M.; Li, X.; Hratchian, H. P.; Izmaylov, A. F.; Bloino, J.; Zheng, G.; Sonnenberg, J. L.; Hada, M.; Ehara, M.; Toyota, K.; Fukuda, R.; Hasegawa, J.; Ishida, M.; Nakajima, T.; Honda, Y.; Kitao, O.; Nakai, H.; Vreven, T.; Montgomery, J. A., Jr.; Peralta, J. E.; Ogliaro, F.; Bearpark, M.; Heyd, J. J.; Brothers, E.; Kudin, K. N.; Staroverov, V. N.; Kobayashi, R.; Normand, J.; Raghavachari, K.; Rendell, A.; Burant, J. C.; Iyengar, S. S.; Tomasi, J.; Cossi, M.; Rega, N.; Millam, J. M.; Klene, M.; Knox, J. E.; Cross, J. B.; Bakken, V.; Adamo, C.; Jaramillo, J.; Gomperts, R.; Stratmann, R. E.; Yazyev, O.; Austin, A. J.; Cammi, R.; Pomelli, C.; Ochterski, J. W.; Martin, R. L.; Morokuma, K.; Zakrzewski, V. G.; Voth, G. A.; Salvador, P.; Dannenberg, J. J.; Dapprich, S.; Daniels, A.

D.; Farkas, O.; Foresman, J. B.; Ortiz, J. V.; Cioslowski, J.; Fox, D. J. *Gaussian 09*, Revision E.01; Gaussian, Inc.: Wallingford, CT, 2013.
(26) Stephens, P. J.; Harada, N. *Chirality* **2009**, *22*, 229−233.
(27) Varetto, U. *MOLEKEL 5.4*; Swiss National Supercomputing Centre: Manno, Switzerland, 2009.

https://dx.doi.org/10.1021/acs.jnatprod.0c00499
J. Nat. Prod. 2020, 83, 3250−3261